Solar Physics
DOI: 10.1007/•••••-•••-•••-••••-•

Article preparation guidelines

Solar Physics

P. Author-a[1] · **E. Author-b**[1] · **M. Author-c**[2]

Abstract The derivation of kinematic profiles for eruptive events is prominent in the field of solar physics. The details on the acceleration of coronal mass ejections (CMEs) and large-scale coronal disturbances ('EIT waves') are important for indicating the driving mechanisms at play. The techniques used for deriving the velocity and acceleration profiles of events based upon the height-time tracks .....

Keywords: CME, EIT Waves, Corona, Mathematical Techniques

1. Introduction

2. Numerical Differentiation Techniques

When presented with a moving object through a sequence of image frames such that it is possible to measure its position at each time step, the technique of numerical differentiation is often used to derive the velocity and acceleration of the object. In the standard 2-point approach, it should be possible to derive the time evolution of a system at time step $t + \Delta t$ according to the system values at time step t. This may be applied through the technique of forward, reverse or centre differencing, resulting in an estimate of the speed of the object at a specific time step given its positional information. More commonly, a 3-point Langrangian interpolation is applied to better approximate the kinematics of a moving object by solving for the Lagrange polynomials that best fit across 3 given datapoints (e.g. DERIV.PRO in IDL). Each of these schemes is based upon the Taylor series expansion of a real function $f(t)$ about the point $t = t_0$:

$$f(t) \;=\; f(t_0) + f'(t_0)(t - t_0) + \frac{f''(t_0)}{2!}(t - t_0)^2 + ... \qquad (1)$$

An alternative form is obtained by letting $t - t_0 = \Delta t$ so that $t = t_0 + \Delta t$ to give:

$$f(t_0 + \Delta t) \;=\; f(t_0) + f'(t_0)\Delta t + \frac{f''(t_0)}{2!}(\Delta t)^2 + ... \qquad (2)$$

[1] First affiliation email: e.mail-a email: e.mail-b
[2] Second affiliation email: e.mail-c

This expansion can be used to determine the numerical derivative of a function according to the choice of technique, detailed in Sections 2.1, 2.2, 2.3 and 2.4 below.

Due to the approximation of an infinite series with a finite number of terms and iterations, an error must be associated with the result, based on its deviation from the true solution. Generally the Euler method is employed, using the formula:

$$y_{n+1} \;=\; y_n + hf(t_n, y_n) \tag{3}$$

to solve the initial value problem $y' = f(t, y)$ given $y(t_0) = y_0$, where h is the stepsize such that $t_n = t_0 + nh$. The convergence of such an approximation to the actual solution is prone to two sources of error; truncation error and round-off error. The truncation error is the difference between the actual solution $y = \phi(t)$ and its numerical approximation based on a finite number of terms in the otherwise infinite series:

$$E_n \;=\; \phi(t_n) - y_n \tag{4}$$

The round-off error is due to the limited precision with which numerical solutions may be found:

$$R_n \;=\; y_n - Y_n \tag{5}$$

where Y_n is the full precision value. The absolute value of the total error is:

$$|E_n + R_n| \;=\; |\phi(t_n) - y_n + y_n - Y_n| \tag{6}$$

$$\leq\; |E_n| + |R_n| \tag{7}$$

Given a function $x = f(u, v)$, the error propagation equation (based on the standard deviations σ of the variables) is written:

$$\sigma_x^2 \;=\; \sigma_u^2 \left(\frac{\partial x}{\partial u}\right)^2 + \sigma_v^2 \left(\frac{\partial x}{\partial v}\right)^2 + 2\sigma_{uv}^2 \left(\frac{\partial x}{\partial u}\right)\left(\frac{\partial x}{\partial v}\right) + ... \tag{8}$$

Specifically in the case of kinematic analyses, this is used to propagate the errors on the height-time data $r(t)$ into the velocity $v(t)$ and acceleration $a(t)$ profiles to determine the associated uncertainties for each technique detailed below. In the case of height-time data the covariance terms are zero because the quantities are uncorrelated.

2.1. Forward Differencing

The forward differencing technique involves extrapolating forward from each time step t to derive the evolution of the system. Thus rewriting Equation 2 to express the distance measurement at time step $t + \Delta t$ gives:

$$r(t + \Delta t) \;=\; r(t) + r'(t)\Delta t + \frac{r''(t)}{2!}(\Delta t)^2 + ... \tag{9}$$

$$\Rightarrow \quad v(t) \equiv r'(t) = \frac{r(t+\Delta t) - r(t)}{\Delta t} + O(\Delta t) \tag{10}$$

where $O(\Delta t)$ is the truncation error term, proportional to the step size Δt between datapoints. It is given as:

$$E = \frac{1}{2} r''(t)\Delta t = \frac{1}{2}\left(\frac{r(t+2\Delta t) - 2r(t+\Delta t) + r(t)}{\Delta t}\right) \tag{11}$$

The forward difference technique inherently assumes that there is a straight-line gradient between points, and its application removes a point from the end of the dataset.

To propagate a one standard deviation uncertainty σ_r of the height data, and σ_t of the time data, into the velocity profile and obtain the associated uncertainty in velocity σ_v, the error propagation equation (Eqn. 8) is written:

$$\sigma_v^2 = \frac{\sigma_{r(t+\Delta t)}^2 + \sigma_{r(t)}^2}{\Delta t^2} + v^2\left(\frac{\sigma_{t+\Delta t}^2 + \sigma_t^2}{\Delta t^2}\right) \tag{12}$$

It is clear that the inverse dependence on Δt^2 will be an important consideration when looking at the effects of measurement cadence for determining kinematics and their associated uncertainties. In effect, reducing the cadence increases the accuracy but decreases the precision (and vice versa) of the derived kinematics.

2.2. Reverse Differencing

The reverse difference technique works in the same manner as the forward difference but is applied at the point $t - \Delta t$ by extrapolating backwards from the point t. This results in:

$$v(t) \equiv r'(t) = \frac{r(t) - r(t-\Delta t)}{\Delta t} + O(\Delta t) \tag{13}$$

where $O(\Delta t)$ is the truncation error term, which, as with the forward difference method, is proportional to the step size Δt between datapoints. It is given as:

$$E = \frac{1}{2} r''(t)\Delta t = \frac{1}{2}\left(\frac{r(t) - 2r(t-\Delta t) + r(t-2\Delta t)}{\Delta t}\right) \tag{14}$$

Similar to forward differencing, the reverse difference technique inherently assumes that there is a straight-line gradient between points, and its application removes a point from the beginning of the dataset.

The error propagation equation for reverse differencing is written:

$$\sigma_v^2 = \frac{\sigma_{r(t)}^2 + \sigma_{r(t-\Delta t)}^2}{\Delta t^2} + v^2\left(\frac{\sigma_t^2 + \sigma_{t-\Delta t}^2}{\Delta t^2}\right) \tag{15}$$

It may be noted that the trends in the derivatives produced by both forward and reverse differencing are identical, the only difference between them being where the resulting profile sits with respect to the time axis.

2.3. Centre Differencing

The centre difference technique uses the two neighbouring points to the point $r(t)$ under examination, i.e., $r(t-\Delta t)$ and $r(t+\Delta t)$, according to the equation:

$$v \equiv r'(t) = \frac{r(t+\Delta t) - r(t-\Delta t)}{2\Delta t} + O(\Delta t)^2 \tag{16}$$

The truncation error in this case is proportional to the square of the step size Δt between datapoints. It is given as:

$$E = \frac{1}{3!} r'''(t)(\Delta t)^2 = \frac{1}{48}\left(\frac{r(t+3\Delta t) - 3r(t+\Delta t) + 3r(t-\Delta t) - r(t-3\Delta t)}{\Delta t}\right) \tag{17}$$

The centre-difference method effectively smoothes the data set while differentiating it by using the two points either side of the point under examination. It is only applicable when the spacing between datapoints is equal, i.e., when Δt remains constant.

The error propagation equation for centre differencing is written:

$$\sigma_v^2 = \frac{\sigma^2_{r(t+\Delta t)} + \sigma^2_{r(t-\Delta t)}}{4\Delta t^2} + v^2\left(\frac{\sigma^2_{t+\Delta t} + \sigma^2_{t-\Delta t}}{4\Delta t^2}\right) \tag{18}$$

2.4. 3-Point Lagrangian Interpolation

3-point Lagrangian interpolation is used in order to determine the first and second derivatives corresponding to the velocity and acceleration of an object specifically when the spacing between datapoints in not equal, i.e., when Δt is non-constant. Considering three data points, (x_0, y_0), (x_1, y_1), (x_2, y_2), the Lagrangian interpolation polynomial is given by:

$$L(x) = \sum_{j=0}^{2} y_j l_j(x) \quad \text{where} \quad l_j(x) = \prod_{i=0, i\neq j}^{2} \frac{x - x_i}{x_j - x_i} \tag{19}$$

The derivative at point x is given by $L' = \partial_x L(x)$. The associated truncation error is given as:

$$E_n = \frac{1}{3!} r'''(t_n)\left(\frac{(t_{n+1} - t_n)^3 + (t_n - t_{n-1})^3}{(t_{n+1} - t_n) + (t_n - t_{n-1})}\right) \tag{20}$$

$$= \frac{1}{3!}\frac{(t_{n+1} - t_n)^3 + (t_n - t_{n-1})^3}{(t_{n+1} - t_{n-1})^2}\left(\frac{1}{t_{n+2} - t_n}\left(\frac{r(t_{n+3}) - r(t_{n+1})}{t_{n+3} - t_{n+1}} - \frac{r(t_{n+1}) - r(t_{n-1})}{t_n - t_{n-2}}\right) - \frac{1}{t_n - t_{n-2}}\left(\frac{r(t_{n+1}\right.\right. \tag{21}$$

The error propagation equation is used to determine the errors on the resulting derivative points in $L' \equiv f(L(x), x)$:

$$\sigma^2_{L'} = \sigma_L^2\left(\frac{\partial L'}{\partial L}\right)^2 + \sigma_x^2\left(\frac{\partial L'}{\partial x}\right)^2 + ... \tag{22}$$

$$= \frac{\sigma_L^2}{\partial x^2} + \frac{\sigma_x^2}{\partial x^2}\left(\frac{\partial L}{\partial x}\right)^2 \tag{23}$$

Or more appropriately written in this context as:

$$\sigma_d^2 = \frac{\sigma_{y_{n+1}}^2 + \sigma_{y_{n-1}}^2}{dx^2} + \frac{\sigma_{x_{n+1}}^2 + \sigma_{x_{n-1}}^2}{dx^2}\left(\frac{dy}{dx}\right)^2 \tag{24}$$

such that the errors on the end points become:

$$\sigma_{d_0}^2 = \frac{9\sigma_{y_0}^2 + 16\sigma_{y_1}^2 + \sigma_{y_2}^2}{(x_2 - x_0)^2} + \frac{\sigma_{x_2}^2 + \sigma_{x_0}^2}{(x_2 - x_0)^2}\left(\frac{3y_0 - 4y_1 + y_2}{x_2 - x_0}\right)^2 \tag{25}$$

$$\sigma_{d_n}^2 = \frac{9\sigma_{y_n}^2 + 16\sigma_{y_{n-1}}^2 + \sigma_{y_{n-2}}^2}{(x_n - x_{n-2})^2} + \frac{\sigma_{x_{n-2}}^2 + \sigma_{x_n}^2}{(x_{n-2} - x_n)^2}\left(\frac{3y_n - 4y_{n-1} + y_{n-2}}{x_{n-2} - x_n}\right)^2 \tag{26}$$

Given three consecutive height-time data points $r(t_1)$, $r(t_2)$, $r(t_3)$, if they are equally spaced such that $\Delta t = |t_1 - t_2| = |t_2 - t_3|$ the resulting error propagation equation when deriving the velocity at t_2 by 3-point Lagrangian interpolation is the same as for centre differencing (Eqn. 18). Otherwise, for unevenly spaced data points it is written:

$$\sigma_v^2 = \frac{\sigma_{r(t_3)}^2 + \sigma_{r(t_1)}^2}{(t_3 - t_1)^2} + v^2\left(\frac{\sigma_{t_3}^2 + \sigma_{t_1}^2}{(t_3 - t_1)^2}\right) \tag{27}$$

3. Models

3.1. Testing for Non-constant Acceleration

For the phenomena of CMEs and other propagating coronal disturbances (e.g. EIT waves), large velocities are reached that indicate early regimes of high acceleration often difficult to quantify due to observational limitations when tracking these diffuse structures (e.g. low cadences and noisy images). Here, we investigate the application of the differencing schemes introduced above for different magnitudes of sampling error, noise and cadence on a non-constant acceleration model of the form:

$$r(t) = \sqrt{10}\left(t\tan^{-1}\left(\frac{e^{t/10}}{\sqrt{10}}\right)\right) \tag{28}$$

If a relatively large cadence is available ($\Delta t = 30$ s) for sampling un-noised data with an assigned error interval of 2% per height measurement, then the kinematic profiles are returned with high precision but low accuracy, making the acceleration regime untestable (Figure 1). Essentially the high cadence acts to smooth out the acceleration peak in the dataset.

If a smaller cadence is available ($\Delta t = 1$ s) for sampling un-noised data with an assigned error interval of 2% per measurement, then the kinematic profiles are returned with near-perfect accuracy but insufficient precision, due to the $(\Delta t)^{-2}$ dependence of the error propagation equations 12, 15 and 18 (Figure 2).

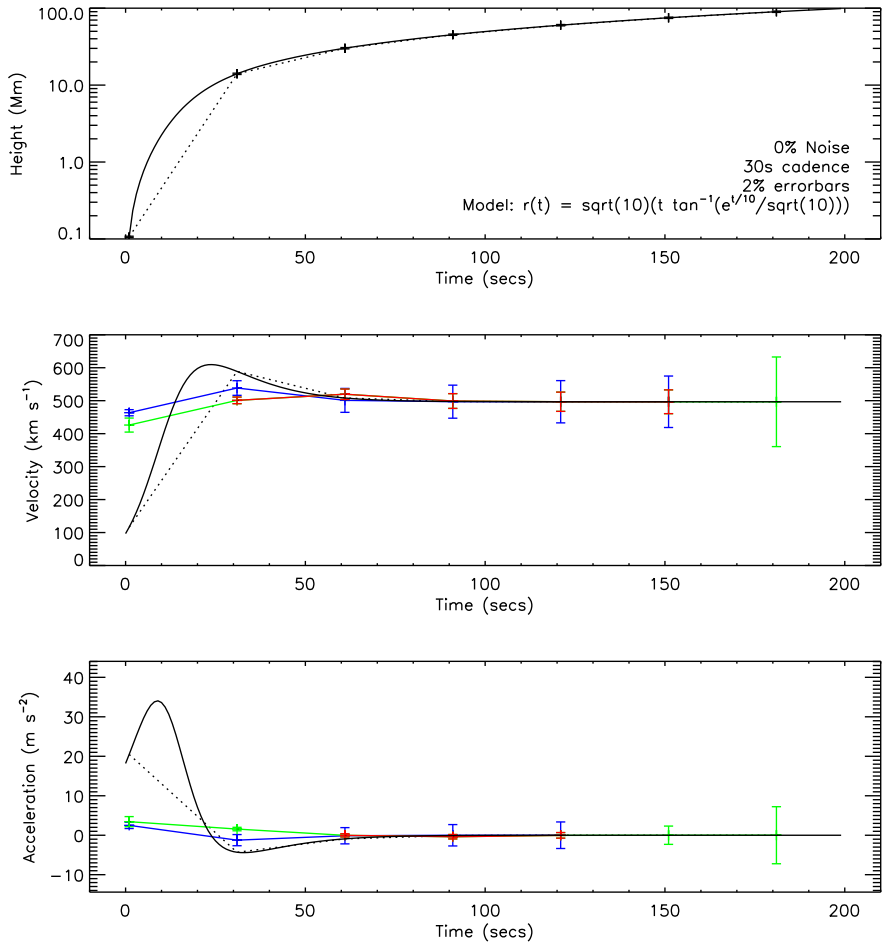

Figure 1. Non-constant acceleration model without noise, at 30 s sampling cadence, with errorsbars at 2% of the data, and the forward, centre and lagrangian differencing techniques applied. Solid black line = Model / Dashed black line = sampled points along model / Blue = Forward / Red = Centre / Green = Lagrangian

We now look toward testing for the acceleration peak in the model dataset for varying cadences, and specifically for the opportune case that we should happen to sample the dataset exactly at the time of maximum acceleration. The model acceleration peak occurs at time $t = 9$ s with the value $a_{model} = 34.04$ m s^{-2}, and the near-perfect accuracy, but low precision, of the differencing schemes (applied to the un-noised data with a sampling cadence of $\Delta t = 1$ s) return comparable values but with large errors: $a_{forward} = 33.55 \pm 90.8$ m s^{-2}, $a_{centre} = a_{lagrangian} = 33.81 \pm 19.8$ m s^{-2}. As the cadence is increased (up to an allowed maximum of $\Delta t = 47$ s on this dataset) the acceleration peak becomes harder to detect and is smoothed out such that its measurement decreases to zero.

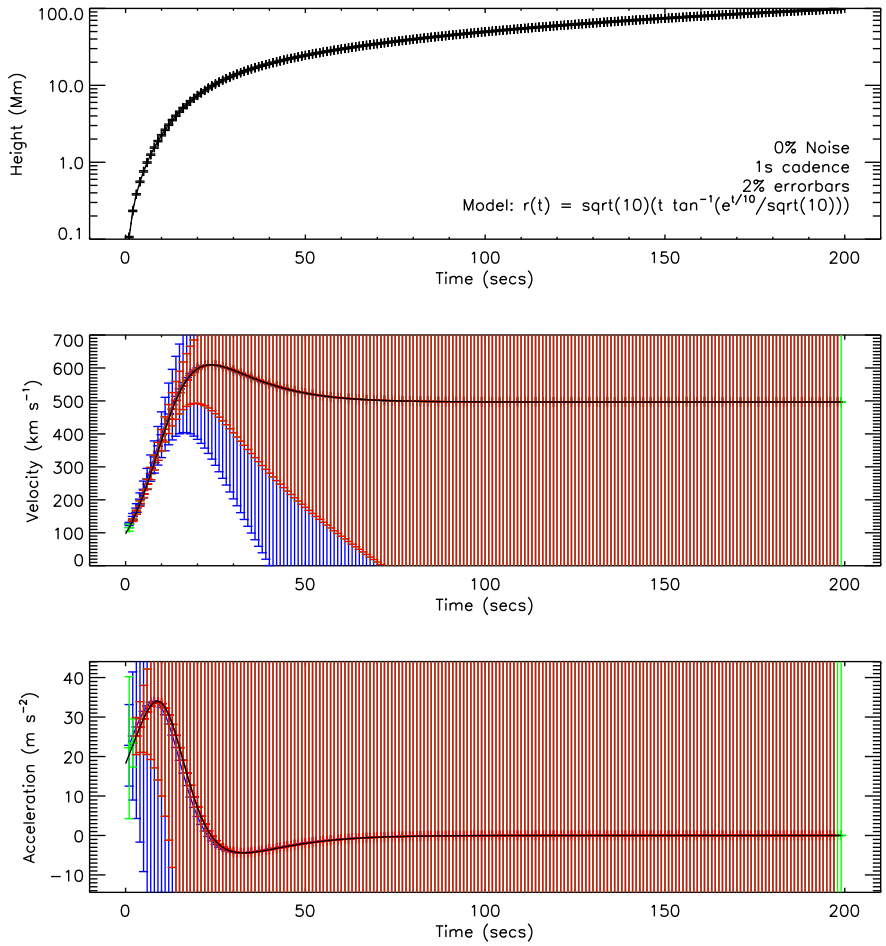

Figure 2. Non-constant acceleration model without noise, at 1 s sampling cadence, with errorsbars at 2% of the data, and the forward, centre and lagrangian differencing techniques applied. Solid black line = Model / Blue = Forward / Red = Centre / Green = Lagrangian

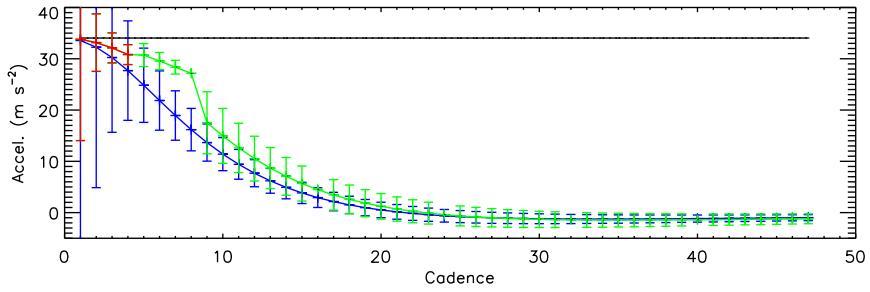

Figure 3. Solid black line = Model peak acceleration / Blue = Forward / Red = Centre / Green = Lagrangian (bug in codes drops every 8th errorbar - to be fixed!)

The addition of noise (of a few percent, say, to represent instrumental effects, human errors, etc.) leads to an increased relative scatter between datapoints, and therefore decreases the accuracy of the derived kinematic profiles. It is imperative that sufficient errorbars be assigned to all measurements on real data, in order to confidently represent the uncertainties involved when determining the kinematics.

4. Data

4.1. CMEs

4.2. EIT waves

5. Bootstrapping

6. Conclusion

Appendix

Acknowledgements The authors thank ... (*note the reduced point size*)

References

Berger, M.A.: 2003, in Ferriz-Mas, A., Núñez, M. (eds.), *Advances in Nonlinear Dynamics*, Taylor and Francis Group, London, 345.
Berger, M.A., Field, G.B.: 1984, *J. Fluid. Mech.* **147**, 133.
Brown, M., Canfield, R., Pevtsov, A.: 1999, Magnetic Helicity in Space and Laboratory Plasmas, Geophys. Mon. Ser. 111, AGU.
Dupont, J.-C., Schmidt, F., Koutny, P.: 2007, *Solar Phys.* **323**, 965.